Available online at www.sciencedirect.com

ScienceDirect

Procedia Structural Integrity 78 (2026) 1197–1204

Structural Integrity Procedia

www.elsevier.com/locate/procedia

XX ANIDIS Conference

Seismic risk reduction of masonry barrel vaults using CRM: fragility assessment using a fiber-section approach

Filippo Campisi[a], Fabio Di Trapani[a,]*, Marielisa Di Leto[a], Calogero Cucchiara[a], Antonio Pio Sberna[b], Lidia La Mendola[a]

[a]*Università degli Studi Di Palermo, Dipartimento di Ingegneria, Viale delle Scienze Ed. 8, 91128, Palermo, Italy*
[b]*Politecnico di Torino, Dipartimento di Ingegneria Strutturale, Edile e Geotecnica, Corso Duca degli Abruzzi 24, 10129, Turin, Italy*

Abstract

Masonry barrel vaults made of calcarenite natural stone are widespread in the built heritage of the Mediterranean area. Post earthquake observations have highlighted their vulnerability under seismic loads especially when they are used as secondary elements carrying their own weight only. This study explores the effectiveness of seismic risk reduction for calcarenite masonry barrel vaults using cementitious reinforced mortar (CRM) in the extrados combined with Glass Fiber Reinforced Polymer (GRFP) grids. A force-based fiber-section beam/column model is implemented to effectively capturing axial force–bending moment interaction while reducing computational costs. Multiple-stripe analyses are carried out for different configurations of the case study based on a real calcarenite masonry barrel vault. The results show that CRM retrofitting can increase displacement capacity and shift fragility curves to higher intensities, with spectral accelerations at 50% collapse probability from two to six times greater than the as-built condition. The influence of additional boundary conditions such as the presence of backfill material and the premature debonding of the reinforcement are also investigated.

Keywords: Masonry vaults, Retrofitting, CRM, Finite Element, Fragility, OpenSees, STKO.

1. Introduction

Masonry barrel vaults are a hallmark of historic architecture worldwide, particularly across the Mediterranean area. Their structural behavior is shaped by multiple factors, including geometry, construction techniques, mass distribution,

* Corresponding author.
E-mail address: fabio.ditrapani@unipa.it

10.1016/j.prostr.2025.12.153

boundary conditions, material degradation, and subsequent alterations. These vaults may serve as structural or non-structural elements. In the first case, usually backfill material is interposed between the vault extrados and the upper floor, which is also sustained by the vault. In the second case the vaults bear only their self-weight, such as ceilings in interior spaces (Boem and Gattesco 2021). Seismic response of masonry barrel vaults has been examined extensively in the literature (Ramaglia et al. 2016, Cardinali et al. 2023) and has attracted attention with respect to different retrofitting solutions to reduce their vulnerability (La Mendola et al 2009, Marini et al. 2017, Gattesco et al. 2018, Boem and Gattesco 2021, Caceres-Vilca et al. 2024). In many cases, composite materials have been adopted for strengthening, owing to their relatively low weight, ease of application, and compatibility with existing substrates. Common solutions include Fiber Reinforced Polymers (FRP), Fiber Reinforced Cementitious Mortars (FRCM), and, more recently, Composite Reinforced Mortars (CRM). Numerical studies were also performed to complement experimental tests using different approaches. In most cases 2D or 3D finite element (FE) models were used (Gattesco et al. 2018, Cardinali et al. 2023, Tanriverdi 2023, Di Leto et al. 2025) adopting the homogenized masonry approach or micro-modelling. On the other hand, the performance of unreinforced and reinforced masonry vaults in the framework of rigorous performance-based earthquake engineering (PBEE) seems missing. Moreover, the adoption of 2D or 3D FE models does not look viable due to the computational cost needed to perform a large number of nonlinear time-history (NLTH) analyses. Recent studies (Raka et al 2015, Di Trapani et al. 2024) have shown the application of 1D beam/column fiber-section elements with a force-based (FB) formulation for nonlinear analyses of masonry building structures, to explicitly consider the axial force – bending moment interaction and overcoming the limitation of concentrated plasticity approaches. In this context this paper proposes a numerical study aimed at the assessment of seismic fragility of masonry barrel vaults in a PBEE probabilistic framework. Fragility assessment is carried out in cases of unreinforced vaults and with CRM coating. In both cases the influence of the backfill material on overall fragility is evaluated. A simplified 1D approach with force-based fiber-section beam/column elements is proposed to model the barrel vaults. The model is developed and validated with the STKO suite for OpenSees/STKO. The results quantify the probability of exceeding the near-collapse limit state for a case study structure and demonstrate the effectiveness of fiber-section-based elements as a reliable and computationally efficient approach.

2. Numerical modelling approach

2.1. Fiber-section-based model formulation

Although barrel vaults are commonly considered as 2D structural elements, their internal stress-state due to gravity and seismic loads can be reconducted to a 1D stress-state. A 1D representation using beam elements with a proper discretization is then viable at least in the elastic stage. On the other hand, masonry vaults as well as arches statics, depends on the axial force (N) / bending moment (M) interaction. Flexural capacity at the section level is increased or decreased if the axial compression varies as in the seismic load cases. Hence modeling of axial force / bending moment coupling is essential for nonlinear static or dynamic analysis.

In the current study fiber-section beam/column elements with force-based formulation are used to reproduce N-M interaction in the nonlinear field. In the force-based formulation section deformations and forces are coupled by the tangent flexibility matrix of the cross-section $\boldsymbol{f}_T^s(x)$ so that:

$$\dot{\boldsymbol{e}}^s(x) = \boldsymbol{f}_T^s(x)\dot{\boldsymbol{s}}^s(x) \tag{1}$$

where $\boldsymbol{f}_T^s(x)$ is a full matrix in the nonlinear case. The vectors $\dot{\boldsymbol{e}}^s(x)$ and $\dot{\boldsymbol{s}}^s(x)$ collect the incremental section deformations (curvature $\dot{\kappa}(x)$ and axial deformation $\dot{\varepsilon}_0(x)$) and forces (moment $\dot{M}(x)$ and axial force $\dot{N}(x)$), namely:

$$\dot{\boldsymbol{e}}^s(x) = \begin{pmatrix} \dot{\kappa}(x) & \dot{\varepsilon}_0(x) \end{pmatrix}^T \quad \dot{\boldsymbol{s}}^s(x) = \begin{pmatrix} \dot{M}(x) & \dot{N}(x) \end{pmatrix}^T \tag{2}$$

Through Eq. (1), force-based approach combined with fiber section elements allow real time updating of the cross-section's flexural resistance as a function of the change internal forces distribution during the analysis. In addition,

fiber-section approach is suitable to model generic shape cross-sections with multiple uniaxial materials under the hypothesis of plane cross sections, making it suitable to model intrados or extrados reinforcement layers.
The vault curved shape can be effectively discretized by using an adequate number of elements (Fig. 1). Considering that the vault is subjected to uniaxial bending, the cross section is discretized in horizontal stripe-shaped fibers. This simplification significantly reduces computational effort without losing in accuracy. The *ASDConcrete1D* (Petracca et al. 2022) damaged-plasticity constitutive model available in the STKO (Petracca et al. 2017) software platform for OpenSees (McKenna et al 2000) is used. This model enables auto-regularization of the fracture energy by computing the specific fracture energy (g_f), which is obtained by scaling the nominal fracture energy (G_f) by the element mesh size (l_{dis}). In the case of force-based fiber-section elements, further adaptation of the fracture energy is required as a function of the selected number of Gauss-Lobatto integration points to prevent strain localization issues. In the present case, given the typically small element size, three Gauss-Lobatto points are used, which needs increasing the specific fracture energy by six times. The modelling approach validation is illustrated in the following section.

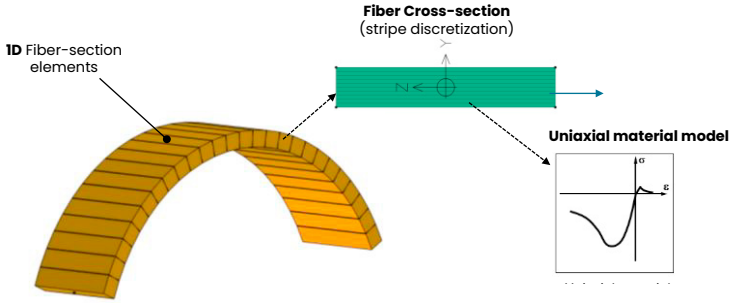

Fig. 1. Proposed 1D fiber-section modelling scheme for the barrel vault.

2.2. Model validation

The proposed modelling approach is validated with the experimental results of a recent experimental quasi-static test on a half-scaled masonry barrel vault specimen (Di Leto et al. 2025, Campisi et al. 2025). The specimen (Fig 2a) was built using calcarenite bricks and a lime-cement mortar. The specimen had a span of 1.92 m and a radius of 1.0 m (Fig. 2b). The calcarenite bricks measured 250×120×50 mm and were laid with the longer sides oriented transversely, resulting in a wall thickness of 120 mm. The mortar joints were 10 mm thick. The overall transverse width of the vault was 1.03 m. The structure was built over two reinforced concrete base supports laterally constrained by the steel columns of the testing frame. The test consisted of the application of a vertical load at a quarter of the span up to the ultimate capacity of the specimen. A picture of the specimen and of the testing setup is illustrated in Fig. 2b.

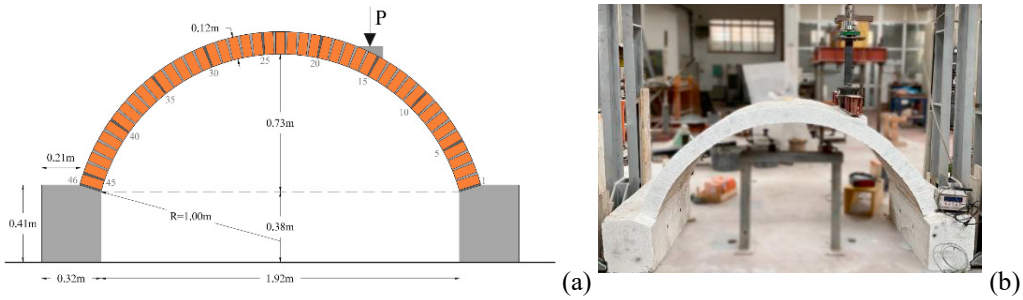

Fig. 2. Calcarenite vault specimen used for validation (Campisi et al. 2025): (a) Geometrical layout of the specimen; (b) View of the specimen within the testing apparatus.

As documented by Campisi et al. 2025, the specimen had a horizontal settlement at one of the concrete supports

causing a delayed achievement of the peak response. The authors were able to retrieve the horizontal reaction at the support as a function of the horizontal displacement (Fig. 3a) and used a zero-length horizonal spring to simulate the test with a refined 2D model of the vault. The same approximation was adopted for the proposed 1D fiber-section modelling approach. A bilinear force-displacement response that was implemented at one of the supports by a *ZeroLength* element using a steel-type (*Steel01*) uniaxial material model (Fig. 3a), while the other support was simply pinned. The vault was discretized into 30 beam elements having a rectangular 1030 x 120 mm cross section with 30 stripes across the thickness. The main mechanical parameters, elastic modulus (E_m), compressive and tensile strength (f_{cm} and f_{mt}), fracture energies in compression and tension (G_c and G_t) for the uniaxial material model are illustrated in Table 1. The comparisons between the experimental and numerical results are illustrated in Fig. (3b) showing quite good agreement. In the same diagram the numerical solution from the refined 2D model by Campisi et al. 2025 is also represented. The comparisons show that the proposed 1D fiber-section has similar performance with respect to the refined 2D model while reducing the analysis time by two orders of magnitude.

Table 1. Mechanical properties used for the numerical model of experimental tests used for the validation.

E_m (MPa)	f_{mc} (MPa)	f_{mt} (MPa)	G_c (N/mm)	G_t (N/mm)
6382	7.36	0.068	8.0	0.024

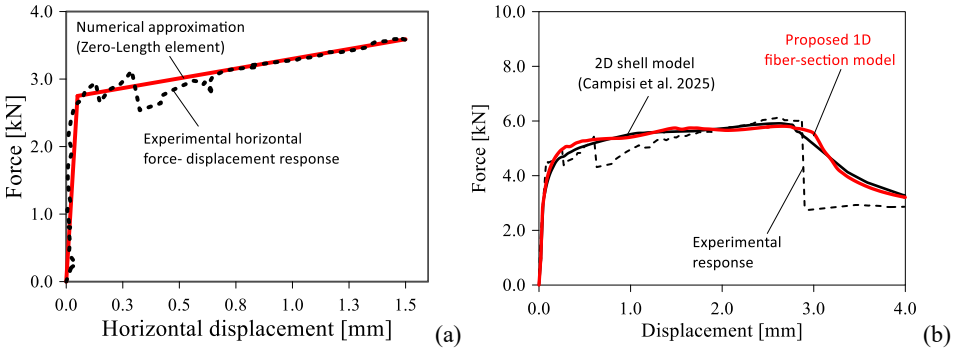

Fig. 3. (a) Relationship between horizontal force and horizontal displacement of the support; (b) Comparison between experimental response of the specimen and numerical simulations with 2D and 1D modelling approaches.

3. Fragility evaluation framework

3.1. Fragility assessment methodology and definition of EDP and IM

Multiple Stripe Analysis (MSA) is used as the reference analysis method for evaluating the probability of exceeding a limit state defined by an engineering demand parameter (EDP) for a given intensity measure (IM), that is:

$$P[EDP \geq EDP_{\lim} \mid IM = x] = \Phi\left(\frac{\ln(x) + \mu_{\ln x}}{\sigma_{\ln x}}\right) \tag{3}$$

In Eq. (3) x is the current value of the intensity measure, Φ is the standard cumulative distribution function, μ_{lnX} and σ_{lnX} are the mean and the standard deviation of the natural logarithms of the distribution of x at the limit EDP (EDP_{lim}). The maximum relative displacement between the top of the vault and the base nodes is assumed as the EDP. It provides a measure of the system's distortion due to the lateral actions, and it's believed to be well correlated with the seismic damage. Since no reference limit EDP are available in the literature, the latter are numerically assessed by a lateral pushover of the vault as it will be shown in the following sections. The spectral acceleration $S_a(T_1)$ is selected as the intensity measure, and the first dominant vibration period of the vault (T_1) is used for conditioning the ground motion set used for the analysis as illustrated in the following section.

3.2. Ground motion selection and MSA intensity scaling criteria

The selection of the ground motion (GM) sets was performed exclusively based on the intensity measure $S_a(T_1)$, evaluated from the reference elastic response spectrum. For a specified T_1, a GM set was selected so that records match the target value of $S_a(T_1)$. The records were chosen from the PEER NGA-West database imposing additional constraints of source-to-site distance ≤ 150 km and magnitude $4.0 \leq M_w \leq 5.0$. To ensure minimal alteration of the original records the selection provided a preliminary screening to identify the records whose $S_a(T_1)$ was already close to the target. Then the records were scaled by small factors in the range [0.90; 1.10] to match the target $S_a(T_1)$. Each set consisted of 20 horizontal unidirectional accelerograms, with no more than three records from the same seismic event. Fig. 4 shows a sample of GM selection for the case of $T_1=0.06$ *s* assuming the NTC 2018 elastic response spectrum of L'Aquila site category B with a return period of 457 years.

To perform the MSA, the GM set was scaled so that the intensity measures IM=$S_a(T_1)$ ranged from 0.10g by 0.10 g increments. Maximum EDPs were extracted at each IM to evaluate the distribution of IM leading to the exceedance of the selected limit state (Fig. 4b). The discrete distributions were fitted with a lognormal model (Baker 2015, Sberna et al. 2025).

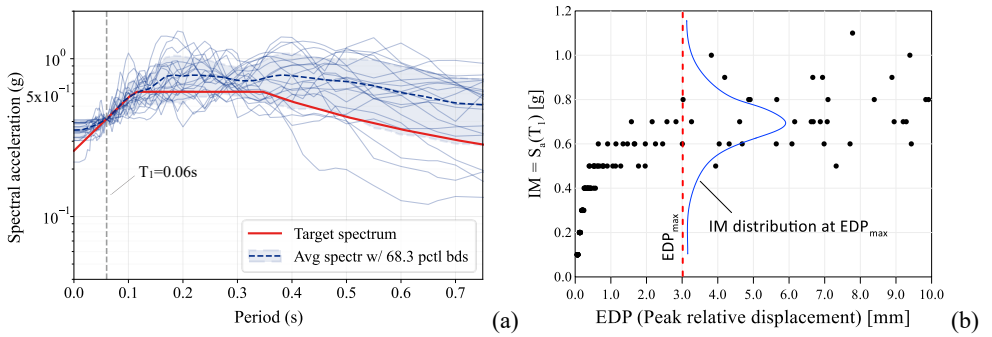

Fig. 4. (a) Sample of GM selection for $T_1=0.06$ *s* and reference target NTC 2018 spectrum; (b) Sample of MSA output.

4. Case study test

4.1. Case study test description and analysis cases

The case study consists of calcarenite masonry building located in Agrigento (Sicily, south of Italy) (Fig. 5) which was formerly used as a hospital and now has changed use to a facility of the University of Palermo. As can be observed from Fig. 5, the building presents several vaulted spans on the mezzanine floor consisting of calcarenite barrel vaults having a span of 4.22 m and a thickness of 180 mm. Data on the masonry, made available by the University of Palermo, provided an average compressive strength f_{mc} of 1.42 MPa and an elastic Young's modulus E_m=3682 MPa.

Fig. 5. Case study test building: main façade, extracted plan and section of the vaulted spans at the mezzanine floor.

Keeping the existing geometry and mechanical properties of the reference cases study vaults, different analysis cases have been defined, and the seismic fragility has been evaluated. In particular, the effect of a 30 mm CRM coating

with a GFRP grid was assessed as well as the influence of the backfill material in the unreinforced and reinforced cases. For the reinforced cases the effect of a prior debonding of the reinforcement was also considered by considering a fictitiously reduced strength for the GFRP. The list of the analysis cases is illustrated in Table 2. The backfill material was considered as an extra weight (18 kN/m^3) and mass to the nodes based on its depth. As regards the CRM reinforcement, the mortar strength was 10 MPa with a tensile strength of 1 MPa and a Young's modulus of 8000 MPa. The nominal strength of the GFRP grid was f_{GFRP}=420.7 MPa (R0). To approximately simulate premature debonding the nominal strength of the GFRP was reduced to 1/2 (R1) and 1/3 (R2).

Table 2. Analysis cases

Case	Description
AB	As-built vault
AB+B	As-built vault + backfill
R0	Retrofitted vault with nominal GFRP tensile strength
R0+B	Retrofitted vault with nominal GFRP tensile strength + backfill
R1	Retrofitted vault with 1/2 GFRP tensile strength
R1+B	Retrofitted vault with 1/2 GFRP tensile strength + backfill
R2	Retrofitted vault with 1/3 GFRP tensile strength
R2+B	Retrofitted vault with 1/3 GFRP tensile strength + backfill

4.2. Numerical model and maximum EDP limit determination

The numerical model of one of the vaults of the case study structure was defined according to the approach described in Section 2. The basic model schemes are illustrated in Fig. 6. For the retrofitted cases (Fig. 6b) the cross-section was defined be adding an extra 40 mm layer representing the mortar coating. Inside the mortar layer a 284 mm^2/m GFRP reinforcement layer was inserted. The latter layer was modelled as an elastic material up to the ultimate tensile or debonding strength. The limit EDPs (EDP$_{max}$) for each configuration were obtained by performing a conventional pushover analysis of the models. An incremental displacement was imposed at the top node up to the achievement system collapse (Fig. 7). The resulting maximum EDPs are illustrated in Table 3 together with the main vibration periods of the models.

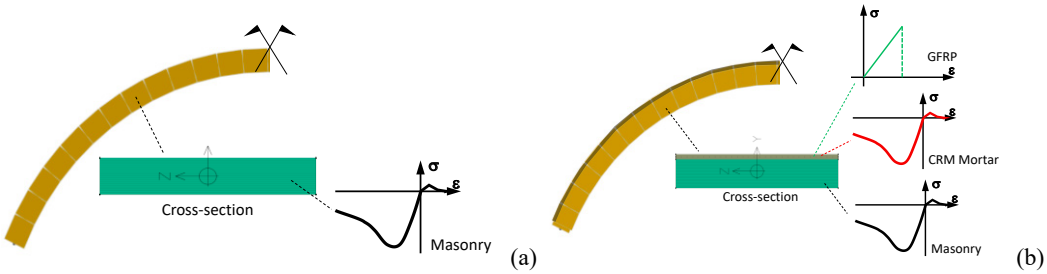

Fig. 6. Case study vault fiber section model samples: (a) Unreinforced cases; (b) Reinforced cases.

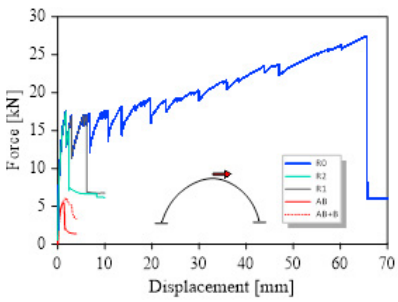

Fig. 7. Conventional pushover analyses of the models for the determination of the maximum EDP (EDP$_{max}$).

Table 3. EDP_{max} and main vibration periods for the case study models.

Case	AB	AB+B	R0	R0+B	R1	R1+B	R2	R2+B
EDP_{max} (mm)	1.3	1.8	67	67	6.0	6.0	2.5	2.5
T_1 (s)	0.05	0.06	0.038	0.043	0.038	0.043	0.038	0.043

4.3. Analysis results

Multiple-stripe analyses were carried out for the considered cases. For each model, the ground motion selection was updated by conditioning the sets to the spectral accelerations at the relevant vibration periods. The target code spectrum shown in Fig. 4a was used as the reference. For the sake of brevity MSA results are illustrated in Fig. 8 only for specimens AB+B and R0+B. In the same diagrams the EDP_{max} are shown for the different case studies. As can be observed, a large increase in the average IM range is obtained for the reinforced case with respect to the as-built condition. The fragility curves are illustrated in Fig. 8 for all the considered case studies. Overall, it is evident that due to the strength and EDP_{max} increment associated with the reinforcement the spectral accelerations at a 50% collapse probability had an increment from two to six times in the retrofitted cases. The backfill material played a dual role. While it had a favorable effect in the non-reinforced cases due to its stabilizing action, its presence increased the fragility of the retrofitted vaults, as the added mass had a major influence. The strength limitation due to the debonding largely reduced the EDP_{max} and the resistance of the retrofitted vaults. However, even in the worse simulated conditions of 1/3 of the nominal GFRP strength, the $S_a(T_1)$ at 50% collapse probability was increased by at least two times. The average collapse $S_a(T_1)$ values are illustrated in Table 4.

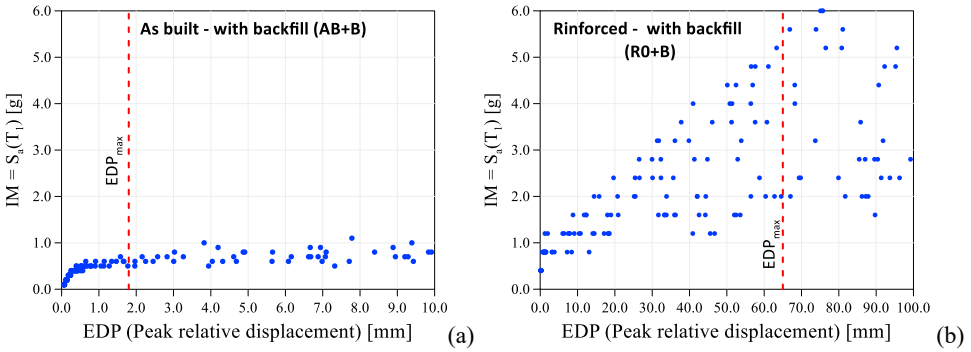

Fig. 8. Multiple Stripe Analysis results: (a) AB+B model; (b) R0+B model.

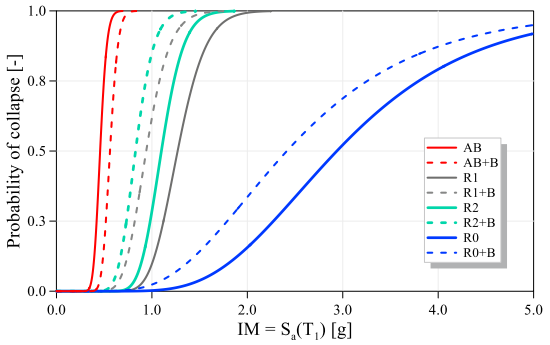

Fig. 9. Fragility curves for the considered cases studies.

Table 4. Average collapse $S_a(T_1)$ values.

Case	AB	AB+B	R0	R0+B	R1	R1+B	R2	R2+B
$S_a(T_1)_{avg}$ [g]	0.46	0.56	3.16	2.66	1.29	0.96	1.12	0.84

5. Conclusions

This study presented a numerical investigation of calcarenite masonry barrel vaults and assessed their seismic fragility with and without extrados CRM reinforcement incorporating GFRP grids. A fiber-section, force-based beam/column formulation was proposed and used to simulate the nonlinear time-history response of unreinforced and reinforced vaults, achieving markedly reduced computational costs. Multiple-stripe analyses on a real case study showed that CRM retrofitting substantially increased EDP_{max} and shifted fragility curves to higher intensities, with $S_a(T_1)$ at 50% collapse probability rising by approximately two to six times compared to the as-built condition. The results also highlighted that the backfill had a dual effect**,** stabilizing unreinforced vaults but increasing the fragility of retrofitted configurations due to added mass. Premature debonding of the grid reduced, yet did not eliminate, the retrofitting benefits. Overall, the findings indicate that CRM strengthening can significantly reduce the seismic vulnerability of masonry barrel vaults, and that the proposed fiber-section approach offers a reliable and efficient tool for PBEE-oriented fragility assessment. Future work should refine material–interface modeling and further investigate the interaction between vaults and the main substructure.

Acknowledgements

This paper was produced with the financial support under the National Recovery and Resilience Plan (NRRP), Mission 4, Component 2, Investment 1.1, funded by the European Union – NextGenerationEU– Project Title: sTructurAl and eneRGy rEnovation for susTainable buildingS - TARGETS – CUP B53D23027280001 Grant Assignment Decree No. 1409 adopted on 14.9.2022 by the Italian Ministry of Ministry of University and Research (MUR).

The authors also thank the University of Palermo for providing the experimental data of the case study.

References

Baker, JW. (2015) Efficient Analytical Fragility Function Fitting Using Dynamic Structural Analysis. Earthquake Spectra. ;31(1):579-599. doi:10.1193/021113EQS025M

Boem, I., Gattesco, N. (2021). Cyclic behavior of masonry barrel vaults strengthened through composite reinforced mortar, considering the role of the connection with the abutments. Engineering Structures, 228, 111518.

Caceres-Vilca, G., Copa-Pineda, J., Copa-Pineda, F., Malaga-Chuquitaype, C. (2024). Experimental assessment of sillar masonry barrel vaults retrofitted with reinforced concrete elements. Structures, 62, 106145.

Campisi, F., Di Leto, M., Di Benedetto, M., Di Trapani, F., Cucchiara, C., & La Mendola, L. (2025). Performance of calcarenite masonry barrel vaults: Experimental investigation and DIC-informed refined numerical simulation. In SAHC 2025: Proceedings of the 14th International Conference on Structural Analysis of Historical Constructions, Lausanne, Switzerland.

Cardinali, V., Pintucchi, B., Tanganelli, M., Trovatelli, F. (2023). Settlement of masonry barrel vaults: An experimental and numerical study. Procedia Structural Integrity, 44, 1252–1259.

Di Leto, M., Campisi, F., Rusticano, G., Cucchiara, C., La Mendola, L. (2025). Experimental and numerical study on masonry barrel vault strengthened through CRM system: Preliminary results. ANIDIS 2025 Conference Proceedings, Perugia, Italy.

Di Trapani, F., Oddo, M.C., Sberna, A.P., La Mendola, L. (2024). Structural health monitoring of masonry structures using stress sensors: Experimental induced damage tests and proposed approach for real-time monitoring. Construction and Building Materials, 449, 138077.

Gattesco, N., Boem, I., Andretta, V. (2018). Experimental behaviour of non-structural masonry vaults reinforced through fibre-reinforced mortar coating and subjected to cyclic horizontal loads. Engineering Structures, 172, 419–431.

La Mendola, L., Failla, A., Cucchiara, C., Accardi, M. (2009). Debonding phenomena in CFRP strengthened calcarenite masonry walls and vaults. Advances in Structural Engineering, 12(5), 745–760.

Marini, A., Belleri, A., Preti, M., Riva, P., Giuriani, E. (2017). Lightweight extrados restraining elements for the anti-seismic retrofit of single-leaf vaults. Engineering Structures, 141, 543–554.

McKenna, F., Fenves, G.L., Scott, M.H. (2000). Open system for earthquake engineering simulation. University of California, Berkeley, CA.

Petracca, M., Camata, G., Spacone, E., Pelà, L. (2022). Efficient constitutive model for continuous micro-modelling of masonry structures. Int. J. Archit. Herit., 17, 1–13.

Petracca, M., Candeloro, F., & Camata, G. (2017a). ASDEA Software STKO user manual.

Raka, E, Spacone, E., Sepe, V., Camata G. (2015). Advanced frame element for seismic analysis of masonry structures: model formulation and validation. Earthq. Eng. Struct. Dyn. 44, 14, 2489-2506.

Ramaglia, G., Lignola, G.P., Prota, A. (2016). Collapse analysis of slender masonry barrel vaults. Engineering Structures, 117, 86–100.

Sberna, A.P., Deb, A., Di Trapani, F., Conte, J.P. (2025). Reliability-based seismic retrofitting design methodology for non-ductile reinforced concrete frame structures, Probabilistic Engineering Mechanics, 103818 doi:10.1016/j.probengmech.2025.103818.

Tanriverdi, S. (2023). An experimental and numerical study of the strengthening of masonry brick vaults. Structures, 47, 800–813.